

# Study of Surface Reactivity of Cobalt Oxides: Interaction with Methanol

Marta Maria Natile and Antonella Glisenti\*

Dipartimento di Chimica Inorganica, Metallorganica ed Analitica, Università di Padova,  
via Loredan, 4-35131 Padova, Italy

Received January 16, 2002. Revised Manuscript Received April 22, 2002

In this paper, the interaction between cobalt oxides ( $\text{Co}_3\text{O}_4$  and  $\text{CoO}$ ) and methanol is studied.  $\text{CoO}$  was obtained by heating under high-vacuum (HV) conditions and characterized by X-ray photoelectron spectroscopy (XPS). The  $\text{Co}_3\text{O}_4$  powder sample was characterized by means of XPS, diffuse reflectance infrared Fourier transform (DRIFT) spectroscopy, X-ray diffraction (XRD), and thermal analysis. The interaction between  $\text{Co}_3\text{O}_4$  and methanol was studied both at atmospheric pressure (by means of DRIFT spectroscopy) and under HV conditions (by means of XPS and quadrupolar mass spectroscopy, QMS), whereas the chemisorption of methanol on the  $\text{CoO}$  surface was studied only under HV conditions. Methanol chemisorbs mainly molecularly on the cobalt oxide surfaces, the alcohol dissociation being more evident at higher temperatures. In the case of  $\text{Co}_3\text{O}_4$ , the formation of formate and polymers of formaldehyde is evident around 473–523 K, whereas under HV conditions, formaldehyde and several decomposition and fragmentation products were observed as well as carbon oxides. Similar results were obtained in the case of  $\text{CoO}$ .

## Introduction

Cobalt oxides are materials that are of interest in several field of applied technology. They have been used in Fischer–Tropsch syntheses<sup>1</sup> and later as hydrodesulfurization catalysts.<sup>2</sup> Currently, cobalt oxides, usually supported on silica, alumina, or silica–alumina mixed oxides, are still employed in catalysis. Cobalt oxides are used as catalysts in the hydrocracking of crude fuels and in several complete oxidation reactions,<sup>3,4</sup> and alumina-supported cobalt–molybdenum systems are commercially important hydrodesulfurization catalysts.<sup>5–8</sup>  $\text{Co}_3\text{O}_4$  shows interesting electrocatalytic properties for some reactions (such as the reduction and evolution of oxygen) that are of great interest (concerning many potential applications in energy conversion). Moreover,  $\text{Co}_3\text{O}_4$  shows the highest catalytic activity for the combustion of CO and of organic compounds, and it can be included in formulations of catalyst for treatment of waste gases<sup>9,10</sup> as well as several Co-containing mixed oxides.

Several papers concerning the interaction between cobalt oxides and oxygen,<sup>11</sup> amines and nitro compounds,<sup>12</sup> CO,  $\text{H}_2$ ,<sup>13</sup>  $\text{NO}$ ,<sup>14</sup>  $\text{CH}_3\text{OH}$ , and  $\text{NH}_3$ <sup>15</sup> are present in the literature. Still, cobalt oxide surface reactivity has not been completely clarified, with particular reference to the evaluation of the distribution of active sites, the interaction mechanisms, and the reaction paths.

In this paper, we focus on the reactivity of  $\text{Co}_3\text{O}_4$  and  $\text{CoO}$  surfaces with respect to methanol. Methanol is an important probe molecule, as it is an intermediate in oxidation reactions; moreover, it is a simple organic molecule characterized by a significant acidity. It is noteworthy that methanol can be either reduced or oxidized by a catalyst and its interaction with an oxide surface can be indicative of the surface acid/base and reduction/oxidation sites.

This paper is part of a comprehensive work<sup>16,17</sup> aiming to understand the reactivity of Co-based mixed-oxide systems, which are very promising in materials technology.

The alcohol was chemisorbed both under atmospheric pressure in nitrogen flow and under high-vacuum (HV) conditions. In the first case, diffuse reflectance infrared

\* Corresponding author.

- (1) Anderson, R. B. *The Fischer–Tropsch Synthesis*; Academic Press: New York, 1984; Chapter 4.
- (2) Gates, B. C.; Katzer, J. R.; Schuit, G. C. A. *Chemistry of Catalytic Processes*; McGraw-Hill: New York, 1979; Chapter 5.
- (3) Castner, D. G.; Watson, Ph. R.; Chan, I. Y. *J. Phys. Chem.* **1989**, *93*, 3188.
- (4) Shirai, M.; Inona, T.; Onishi, H.; Asakura, K.; Iwasawa, Y. *J. Catal.* **1994**, *145*, 159.
- (5) Delvaux, G.; Grange, P.; Delmon, B. *J. Catal.* **1979**, *56*, 991.
- (6) Alstrup, I.; Chorkendorff, I.; Candia, R.; Clausen, B. S.; Topsoe, H. *J. Catal.* **1982**, *77*, 397.
- (7) Kasztelan, R.; Toulhout, H.; Grimblot, J.; Bonnelle, J. P. *Appl. Catal.* **1984**, *13*, 127.
- (8) Chin, R.; Herculus, D. M. *J. Phys. Chem.* **1982**, *86*, 3079.
- (9) Spivey, J. J. *Ind. Eng. Chem. Res.* **1987**, *26*, 2165.
- (10) Barresi, A.; Mazzarino, I.; Ruggeri, B. *Chim. Ind.* **1989**, *71*, 64.

- (11) Jeng, S. P.; Zhang, Z.; Henrich, V. E. *Phys. Rev. B* **1991**, *44*, 3266.
- (12) Meijers, S.; Ponec, V. *J. Catal.* **1994**, *149*, 307.
- (13) Gamboa Mutuberria, I.; Guil, J. M.; Ruiz Paniego, A. *Ber. Bunsen-Ges. Phys. Chem.* **1995**, *97*, 77.
- (14) Hassel, M.; Freund, H.-J. *Surf. Sci.* **1995**, *325*, 163.
- (15) Busca, G.; Guidetti, R.; Lorenzelli, V. *J. Chem. Soc., Faraday Trans.* **1990**, *86*, 989.
- (16) Natile, M. M.; Glisenti, A. Study of the surface reactivity of  $\text{NiO}$ : interaction with methanol. *Chem. Mater.*, manuscript submitted.
- (17) Natile, M. M.; Glisenti, A. Study of the surface reactivity of Ni–Co–Fe oxide based nanocomposite catalysts: interaction with methanol. *Chem. Mater.*, manuscript submitted.

Fourier transform (DRIFT) spectroscopy was used for characterization, whereas under HV conditions, the interaction was studied by means of X-ray photoelectron spectroscopy (XPS) and quadrupolar mass spectrometry (QMS). The possibility of operating under HV conditions allows the effect of the distributions of the oxygen and hydroxyl groups on the oxide surface reactivity to be investigated. The importance of OH groups with Brønsted acid character, of active oxygen sites, or of O vacancy points on the catalyst reactivity is well-known.<sup>11,13,14,18</sup>

It is noteworthy that both the HV experiment and the atmospheric-pressure one were carried out avoiding any activation or cleaning treatment. The effect of the activation/cleaning procedures on the surface reactivity will be the subject of following papers.

CoO was prepared under HV conditions, and its reactivity with respect to the alcohol was investigated and compared with that of Co<sub>3</sub>O<sub>4</sub>.

## Experimental Session

**(a) Co<sub>3</sub>O<sub>4</sub> Preparation.** The catalyst was prepared by precipitation from a basic solution of Co(NO<sub>3</sub>)<sub>2</sub>·6H<sub>2</sub>O (Sigma Aldrich, 98%). The solution was obtained by dissolving the nitrate in bidistilled water and adding NH<sub>4</sub>OH (Carlo Erba, water solution 30%) until pH 8–9.

The precipitated Co(OH)<sub>2</sub> was filtered out and washed with bidistilled water until pH = 7; then, it was dried at 573 K for 10 h and calcined in air at 1023 K for 20 h.

The powder used for the DRIFT analysis was kept in nitrogen flow to eliminate water traces until a stable IR spectrum was obtained.

Before chemisorption in HV, the sample was processed as a pellet (the powder was pressed at ca. 2 × 10<sup>8</sup> Pa for 10 min) and evacuated at 1 × 10<sup>-3</sup> Pa for 12 h.

**(b) Reaction Conditions.** Methanol (HPLC-grade) for chemisorption experiments (Sigma-Aldrich, >99.9%) was used without further purification.

The exposure of the pellet to methanol under HV conditions was carried out at temperatures ranging from room temperature (RT) to 773 K at a total pressure of ca. 4–5 × 10<sup>-4</sup> Pa. Alcohol vapors were obtained by evaporation under vacuum. The HV reactor, directly connected to the XPS analysis chamber, allows us to work in flow conditions. The temperature of the pellet was evaluated by means of a thermocouple directly in contact with the sample holder. The volatile products were characterized by means of a quadrupole gas analyzer (European Spectrometry Systems, ESS). The QMS spectra were obtained by subtracting from the spectrum recorded after chemisorption the one obtained just before. Desorption patterns were obtained from the mass spectra by plotting the intensities (partial pressures) of the different masses as a function of temperature.

Mass spectra assignments were made in reference to the fragmentation patterns.<sup>19</sup> Moreover, all mass data were analyzed by using the method proposed by Ko et al.<sup>20</sup>

The exposure of powder samples to methanol in the FTIR equipment was done by using the Spectra-Tech, Inc., COLLECTOR apparatus for diffuse reflectance

infrared Fourier transform (DRIFT) spectroscopy fitted with an HTHP (high-temperature high-pressure) chamber. The HTHP chamber was filled with nitrogen vapors flowing through a bubbler containing the alcohol.

**(c) DRIFT Measurements.** IR spectra were obtained by means of a Bruker IFS 66 spectrometer working in diffuse reflectance mode and are displayed in Kubelka–Munk units.<sup>21,22</sup> The resolution of the spectra was 4 cm<sup>-1</sup>. The sample temperature was measured through a thermocouple inserted into the sample holder directly in contact with the powder.

**(d) XPS Measurements.** XP spectra were recorded using a Perkin-Elmer PHI 5600 ci spectrometer with standard Al K $\alpha$  and Mg K $\alpha$  sources (1486.6 and 1253.6 eV, respectively) working at 350 W. The working pressure was less than 1 × 10<sup>-8</sup> Pa. The spectrometer was calibrated by assuming the binding energy (BE) of the Au 4f<sub>7/2</sub> line to be 84.0 eV with respect to the Fermi level. Extended spectra (survey) were collected in the range 0–1350 eV (187.85-eV pass energy, 0.4-eV step, 0.05 s·step<sup>-1</sup>). Detailed spectra were recorded for the following regions: C 1s, O 1s, and Co 2p (23.5-eV pass energy, 0.1-eV step, 0.1 s·step<sup>-1</sup>). The standard deviation in the BE values of the XPS line is 0.10 eV. The atomic percentage, after a Shirley-type background subtraction,<sup>23</sup> was evaluated using the PHI sensitivity factors.<sup>24</sup> To account for charging problems, the C 1s peak was considered to be located at 285.0 eV, and the peak BE differences were evaluated.

**(e) Thermal Analysis and XRD.** Thermogravimetric analysis (TGA) and differential scanning calorimetry (DSC) were carried out in a controlled atmosphere using the simultaneous differential technique (SDT) 2960 of TA Instruments. Thermograms were recorded at 4 and 10 °C min<sup>-1</sup> heating rates in air and in nitrogen flow. The covered temperature ranged from RT to 1273 K.

XRD patterns were obtained with a Philips diffractometer with Bragg–Brentano geometry using Cu K $\alpha$  radiation (40 kV, 40 mA,  $\lambda$  = 0.154 nm).

## Results

**(a) Co<sub>3</sub>O<sub>4</sub> Characterization.** The catalyst powder was characterized by means of XRD, DRIFT, and XP spectroscopic techniques as well as thermal analysis. The effect of the calcination temperature was investigated by comparing the results obtained on powder samples heated at 573 and 1023 K.

The XRD peak positions observed in the sample treated at 1023 K (consistent with a spinel structure) differ slightly from the tabulated values (Table 1). The average crystallite diameter is about 82 nm;<sup>25</sup> it is noteworthy that the peak shape also suggests the presence of smaller crystallites.

(19) Lias, S. G.; Stein, S. E. *NIST/EPA/MSDC Mass Spectral Database*, PC version 3.0; National Institute of Standards and Technology: Gaithersburg, MD, 1990.

(20) Ko, E. I.; Benzinger, J. B.; Madix, R. J. *J. Catal.* **1980**, 62, 264.

(21) Kubelka, P.; Munk, F. *Z. Tech. Phys.* **1931**, 12, 593.

(22) Kortum, G. *Reflectance Spectroscopy*; Springer: New York, 1969.

(23) Shirley, D. A. *Phys. Rev.* **1972**, 55, 4709.

(24) Moulder, J. F.; Stickle, W. F.; Sobol, P. E.; Bomben, K. D. In *Handbook of X-ray Photoelectron Spectroscopy*; Chastain, J., Ed.; Physical Electronics: Eden Prairie, MN, 1992.

(25) Enzo, S.; Polizzi, S.; Benedetti, A. *Z. Kristallogr.* **1985**, 170, 275.

**Table 1. XRD Data<sup>a</sup> Obtained for Co<sub>3</sub>O<sub>4</sub> Compared to JCPDS Card**

Co <sub>3</sub> O <sub>4</sub> <sup>b</sup>	Co <sub>3</sub> O <sub>4</sub> <sup>c</sup>	Co <sub>3</sub> O <sub>4</sub> <sup>d</sup>
2.431 (100)	2.437 (100)	2.4374 (100)
2.851 (30)	2.858 (34)	2.858 (33)
1.427 (38)	1.429 (34)	1.4291 (38)
1.553 (32)	1.5557 (29)	1.5557 (32)
2.017 (23)	2.021 (19)	2.021 (20)

<sup>a</sup> Crystallographic plane distances, nm. <sup>b</sup> This work. <sup>c</sup> Joint Committee on Powder Diffraction Standards card number JCPDS 42-1467. <sup>d</sup> Joint Committee on Powder Diffraction Standards card number JCPDS 43-1003.

The XP Co 2p<sub>3/2</sub> and 2p<sub>1/2</sub> peak positions (Table 2 and Figure 1) agree with the presence of Co<sub>3</sub>O<sub>4</sub><sup>24,26</sup> both in the sample treated at 573 K for 10 h and in the sample calcined at 1023 K; the almost complete absence of the shake-up peaks characteristic of the Co(II) in CoO<sup>14,27</sup> is even more indicative of this situation. Co(II) and Co(III) oxides can be differentiated in XPS using their different magnetic properties. In fact, the XP spectra of Co(II) high-spin compounds, such as CoO, are characterized by an intense shake-up satellite structure at ca. 787.0 and 804.0 eV. Unlike in Co(II) compounds, in the low-spin Co(III) compounds, the satellite structure is weak or missing.<sup>28,29</sup> Co<sub>3</sub>O<sub>4</sub>, a mixed-valence oxide, shows a weak satellite structure symptomatic of shake-up from the minor Co(II) component.<sup>30</sup>

The O 1s XP peak obtained for the Co<sub>3</sub>O<sub>4</sub> powder calcined at 1023 K is shown in Figure 2; the asymmetry of the O 1s peak on its higher-BE side suggests the presence of surface hydroxyl groups. The O 1s peak fitting procedure shows, for the sample treated at 1023 K, three contributions centered around 530.3, 531.4, and 532.8 eV. The peak at 530.3 eV is attributed to the Co—O bonds, and the other two bands suggest the presence, on the Co<sub>3</sub>O<sub>4</sub> surface, of nonequivalent hydroxyl groups (or of chemisorbed water).<sup>28</sup>

The heat treatment does not influence the Co 2p or O 1s XP peak positions and shapes observed for the powder. The O/Co atomic ratio, in contrast, is 1.1 in the powder sample heated at 573 K and 1.4 in the samples heated at 1023 K.

The DRIFT spectra recorded at RT for the Co<sub>3</sub>O<sub>4</sub> powder samples calcined at 573 and 1023 K are reported in Figure 3. The spectra show two very strong signals at ca. 695–698 cm<sup>-1</sup> and 610–613 cm<sup>-1</sup> (Figure 3a) attributed to the longitudinal vibrations.<sup>31,32</sup> The only contributions in the O—H stretching region can be observed for the sample calcined at 573 K (Figure 3b). Two peaks at 3630 and 3550–3590 cm<sup>-1</sup> are attributed to the presence of H-bonded hydroxyl groups,<sup>32–35</sup> and

(26) *X-ray Photoelectron Spectroscopy Database 20*, version 3.0; National Institute of Standards and Technology: Gaithersburg, MD.

(27) Oku, M.; Hirokawa, K. *J. Electron Spectrosc. Related Phenom.* **1976**, *8*, 475.

(28) Briggs, D.; Riviere J. C. In *Practical Surface Analysis*; Briggs, D., Seah, M. P., Eds.: New York, Wiley: 1983.

(29) Schenck, C. V.; Dillard, J. G.; Murray, J. W. *J. Colloid Interface Sci.* **1983**, *95*, 398.

(30) McIntyre, N. S.; Cook, M. G. *Anal. Chem.* **1975**, *47*, 2208.

(31) Lefez, B.; Nkeng, P.; Lopitaloux, J.; Poillerat, G. *Mater. Res. Bull.* **1996**, *31*, 1263.

(32) Nkeng, P.; Koenig, J.-F.; Gautier, J. L.; Chartier, P.; Poillerat, G. *J. Electroanal. Chem.* **1996**, *402*, 81.

(33) Ramis, G.; Busca, G.; Cristiani, C.; Lietti, L.; Forzatti, P.; Bregani, F. *Langmuir* **1992**, *8*, 1744.

(34) Little, L. H. In *Infrared Spectra of Adsorbed Species*; Academic Press: San Diego, CA, 1966; Chapter 3.

a broad band between 3300 and 3500 cm<sup>-1</sup> suggests the presence of water molecules chemisorbed on the sample surface.<sup>34–36</sup>

The DRIFT spectra of the samples calcined at 573 K have been recorded at increasing temperatures from RT to 523 K. The sample heating causes abrupt decreases of the contributions at ca. 3300–3500 and 3550–3590 cm<sup>-1</sup>, whereas the peak centered at ca. 3630 cm<sup>-1</sup> seems to resist to the temperature increment; this result suggests a different behavior of the two hydroxyl groups with respect to the heat treatment.

Thermal analysis results are shown in Figure 4; the thermal spectra were recorded both in N<sub>2</sub> and in air flow, and different results were obtained (Figure 4a). Inspection of the thermal spectra measured in air flow shows a significant weight loss around 1181 K corresponding to the decomposition of Co<sub>3</sub>O<sub>4</sub> to CoO; in N<sub>2</sub>, Co<sub>3</sub>O<sub>4</sub> decomposes at lower temperature (around 1033 K) (Figure 4a). Moreover, the heat flow is higher in air. The thermal analysis results are different for the samples treated at 573 and 1023 K (Figure 4b). In accordance with the DRIFT results, the sample heated at 573 K shows a significant water loss at low temperatures and a weight decrease due to the condensation of OH groups until about 813 K (Figure 4b). At higher temperatures, the only significant weight change is due to the already mentioned decomposition of Co<sub>3</sub>O<sub>4</sub> to CoO. In contrast, for the sample calcined at 1023 K (Figure 4b), the weight loss due to the water desorption or to OH group condensation is almost insignificant, confirming the data obtained by means of XP and DRIFT spectroscopic techniques. It is noteworthy that only XPS reveals the presence of surface OH groups on the sample calcined at 1023 K; this result is not at variance with the DRIFT spectroscopy and thermal analysis data because the surface-specificity of photoelectron spectroscopy must be considered.

Moreover, water loss is quite low for Co<sub>3</sub>O<sub>4</sub>; other oxides, such as NiO<sup>16</sup> or Fe<sub>2</sub>O<sub>3</sub>,<sup>37,38</sup> show higher degrees of surface hydroxylation. The reactivity toward methanol was studied for the Co<sub>3</sub>O<sub>4</sub> powder sample treated at 1023 K.

**(b) Reaction with Methanol: Atmospheric Pressure Conditions.** DRIFT spectra obtained after the exposure of the Co<sub>3</sub>O<sub>4</sub> powder sample to methanol at temperatures ranging from RT to 523 K are shown in Figures 5 and 6, and in Table 3, the IR data concerning liquid- and gas-phase methanol, as well as some methoxy species, are reported.

In the DRIFT spectra, the presence of gas-phase methanol is suggested by the characteristic P, Q, and R rotational branches in the C—O stretching region at 1054, 1032, and 1016 cm<sup>-1</sup> (Figure 5a, peaks a–c) and is confirmed by the C—H stretching contributions (Figure 5b, peaks g and f).<sup>39,40</sup> In the O—H stretching

(35) Boehm, H.-P.; Knözinger, H. In *Catalysis—Science and Technology*; Anderson, J. R., Boudart, M., Eds.; Springer-Verlag: 1983; Vol. 4, Chapter 2.

(36) Nazri, G.; Corrigan, D. A.; Maheswari, S. P. *Langmuir* **1989**, *5*, 17.

(37) Glisenti, A.; Favero, G.; Granozzi, G. *J. Chem. Soc., Faraday Trans.* **1998**, *94*, 173.

(38) Glisenti, A. *J. Chem. Soc., Faraday Trans.* **1998**, *94*, 3671.

(39) Falk, M.; Whalley, E. *J. Chem. Phys.* **1961**, *34*, 1554.

(40) Herzberg, G. *Infrared and Raman Spectra of Polyatomic Molecules*; Van Nostrand: New York, 1949.

**Table 2. XPS Peak Positions (BE in eV) Obtained for the  $\text{Co}_3\text{O}_4$  Powder as a Function of the Calcination Temperature, Compared with the Literature Values<sup>a</sup>**

sample (calcination temperature/K)	Co 2p <sub>3/2</sub>	shake-up Co 2p <sub>3/2</sub>	Co 2p <sub>1/2</sub>	shake-up Co 2p <sub>1/2</sub>
573	780.0		795.4	803.2
1023	780.3		795.5	804.6
$\text{Co}_3\text{O}_4$	780.0–780.3 <sup>27,71–73</sup>	789.3 <sup>72</sup>	795.4 <sup>27</sup>	804.9 <sup>27</sup>
CoO	780.4–781.1 <sup>14,27,50,72</sup>	787.0, 787.3 <sup>14,26</sup>	796.0, 796.2 <sup>14,27</sup>	804.0, 802.5 <sup>14,27</sup>

<sup>a</sup> Values observed for CoO are also shown.

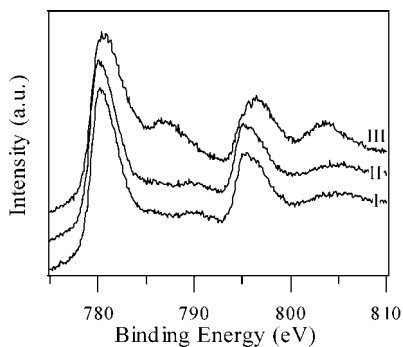


**Figure 1.** Co 2p XP spectra obtained on the  $\text{Co}_3\text{O}_4$  powder (calcined at 1023 K) (I) before and after the exposure to methanol at (II) RT and (III) 773 K. (The spectra are normalized with respect to their maximum values.)

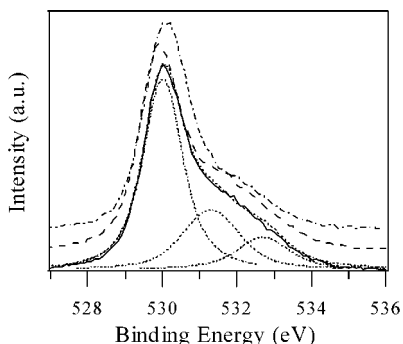


**Figure 2.** O 1s XP spectra obtained on the  $\text{Co}_3\text{O}_4$  powder (calcined at 1023 K) (—) before and after the exposure to methanol at (---) RT and (---) 773 K. (The spectra are normalized with respect to their maximum values; the fitting procedure results are also shown.)

region (Figure 5c), weak peaks at 3663, 3679, 3700, and 3714  $\text{cm}^{-1}$  (peaks i), which are characteristic of gaseous methanol,<sup>39,40</sup> can be observed. The peaks for gaseous methanol decrease with increasing temperature.

At 373 K, a shoulder can be observed in the C–O stretching region around 1061  $\text{cm}^{-1}$  (Figure 5a, shoulder d) that becomes more and more evident as temperature increases; this new contribution might be due to the formation of methoxy groups<sup>37,41</sup> as a consequence of alcohol dissociation on the powder surface. Consistently, in the O–H stretching region, new peaks around 3500, 3600, and 3844  $\text{cm}^{-1}$  appear, suggesting the formation of H-bonded and isolated hydroxyl groups (Figure 5c, peaks l and m, respectively).<sup>34,35</sup>

At higher temperatures (423 K), a broad band becomes visible between 3200 and 3650  $\text{cm}^{-1}$  (Figure 5c, band n) and increases with the temperature. This broad band can be attributed to the O–H stretching vibrations of molecularly chemisorbed water.<sup>34,35,37,38,42</sup> The presence of molecularly chemisorbed water on the powder surface is also confirmed by the O–H bending peak at 1636  $\text{cm}^{-1}$ .

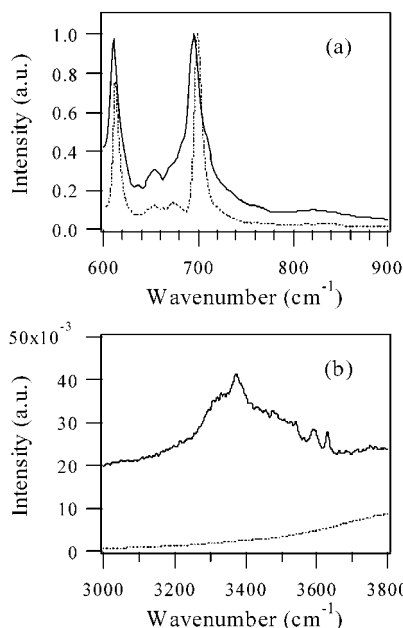


**Figure 3.** DRIFT spectra of the  $\text{Co}_3\text{O}_4$  catalyst powder obtained after the heat treatment at (—) 573 and (---) 1023 K: (a) region between 600 and 900  $\text{cm}^{-1}$ , (b) O–H stretching region.

At 523 K, the peaks around 3844  $\text{cm}^{-1}$  (Figure 5c, peaks m) become more evident, suggesting the increased formation of free OH groups.<sup>34,35,37,38</sup>

The C–H stretching region (Figure 5b) shows a complex shape, in agreement with the presence of several species (gaseous and molecularly chemisorbed methanol, methoxy groups, etc.).<sup>34–42</sup>

Small peaks around 1150, 1165, 1187, 1235, 1280, and 1300  $\text{cm}^{-1}$  (Figure 6a) and at 995–1000 and 974–978  $\text{cm}^{-1}$  (Figure 5a) suggest the formation of dioxymethylene at 373 K, followed, at 423 K, by the formation of polyoxymethylene.<sup>43,44</sup>

At temperatures higher than 373 K, new peaks in the region between 1310 and 1560  $\text{cm}^{-1}$  (Figure 6b) suggest the formation of formate. In fact, the signals at 1360 (peak a) and 1521 (peak b)  $\text{cm}^{-1}$  can be assigned to symmetric and asymmetric O–C–O stretching.<sup>34,37,38</sup>

It is noteworthy that a nitrogen flow is sufficient to remove all of the species from the cobalt oxide surface exposed to methanol at RT (Figure 7); only when the exposure is carried out at high temperatures (473–523 K) do water (Figure 7a, band n), formate (Figure 7b, peaks a and b), and traces of polymers (Figure 7b) remain visible on the powder surface after the nitrogen

(41) Greenler, R. G. *J. Chem. Phys.* **1962**, *37*, 2094.

(42) Glisic, A. *J. Mol. Catal. A: Chem.* **2000**, *153*, 169.

(43) Busca, G.; Lamotte, J.; Lavalle, J.-C.; Lorenzelli, V. *J. Am. Chem. Soc.* **1987**, *109*, 5197.

(44) Jugnet, Y.; Minh Duc, T. *J. Phys. Chem. Solids* **1979**, *40*, 29.

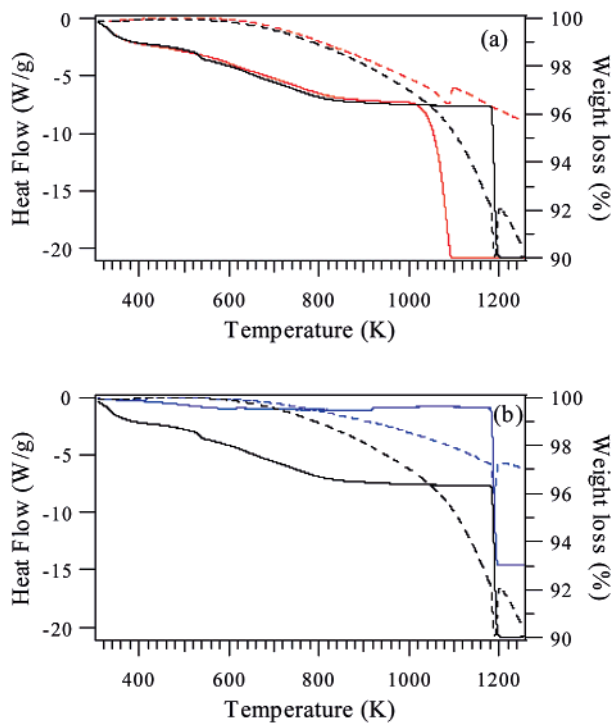


**Figure 4.** TGA and DSC spectra (solid and broken lines, respectively) obtained on the  $\text{Co}_3\text{O}_4$  powder: (a) thermal analysis spectra recorded in (red) nitrogen and (black) in air flow of the sample heated at 573 K; (b) thermal analysis spectra obtained in air flow on the samples heated at (black) 573 and (blue) 1023 K.

flow. Also, the peaks around  $3844\text{ cm}^{-1}$ , attributed to the presence of free OH groups, cannot be eliminated by the nitrogen flow (Figure 7a, peaks m).

Another important point is that the DRIFT spectra never reveal the formation of carbon oxides. Summarizing, at RT, methanol interacts with the  $\text{Co}_3\text{O}_4$  surface mainly molecularly; the alcohol dissociation is significant at  $T \geq 373\text{ K}$ . Around 373 K, the formation of dioxymethylene is evident, whereas around 423–523 K, formate and polymers of formaldehyde prevail; these species interact more strongly than methanol with the oxide surface and do not decompose significantly to carbon oxides.

**(c) Reaction with Methanol: HV Conditions.** The Co 2p and O 1s XP spectra obtained after exposure of  $\text{Co}_3\text{O}_4$  powder to methanol at RT are shown in Figures 1 and 2. The Co 2p and the O 1s peak positions and shapes do not change significantly after the chemisorption at RT, whereas the O 1s peak high-BE tail decreases after exposure to the alcohol at high temperatures. The O/Co atomic ratio decreases from 1.4 to 1.2 after methanol chemisorption at RT and reaches a value of 0.9 after exposure to methanol at 773 K. The surface reduction is a consequence of several phenomena: the interaction between the methanol and the surface, the reaction path, and the heat treatments under HV conditions.

The QMS data (Figure 8) show the desorption of molecularly chemisorbed methanol ( $m/e = 31$ )<sup>19,37,42,45,46</sup> at temperatures lower than about 373 K, suggesting a weaker interaction than the case of nickel oxide in which the desorption of the molecularly chemisorbed methanol occurs up to higher temperature (423 K).<sup>16</sup> At 473 and

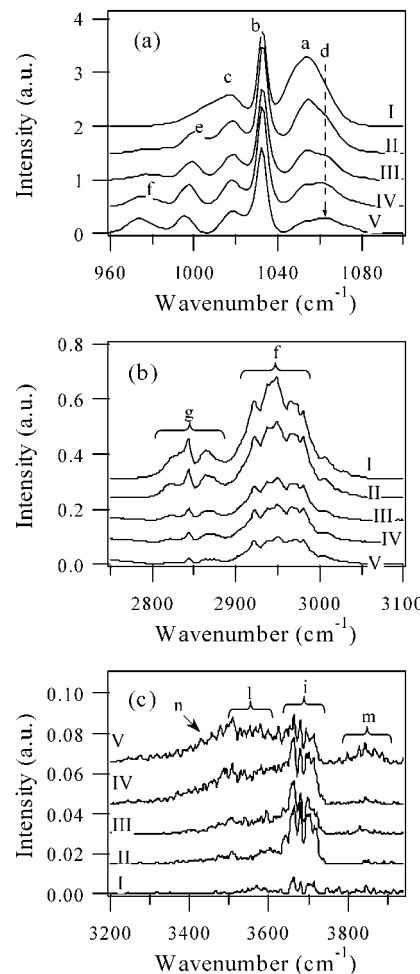


**Figure 5.** DRIFT spectra (Kubelka–Munk units) obtained after exposure of the  $\text{Co}_3\text{O}_4$  powder (calcined at 1023 K) to methanol at different temperatures: (I) RT, (II) 373 K, (III) 423 K, (IV) 473 K, (V) 523 K. (a) C–O stretching region, (b) C–H stretching region, (c) O–H stretching region.

573 K, the methoxy groups desorb<sup>19</sup> as a consequence of the recombination reaction of hydroxyls and alkoxide species.<sup>37,42,47</sup>

The QMS spectra also show the presence of CO,  $\text{CO}_2$ ,  $\text{H}_2\text{O}$ , and  $\text{H}_2$  ( $m/e = 28, 44, 18$ , and 2, respectively) and of several fragmentation and recombination products.<sup>19,37,42,46</sup>

Molecularly chemisorbed methanol desorption is accompanied by the desorption of  $\text{CO}_2$  and of fragmentation/recombination products (methyl ether and ethyl methyl ether).<sup>46,47</sup> At 473 K, the methoxy groups desorb and decompose to CO and  $\text{H}_2\text{O}$ . At higher temperatures, the methoxy group desorption is accompanied mainly by the presence of CO.<sup>47</sup> The fragmentation/recombination path always competes with the desorption and oxidation of methanol.

**(d) Synthesis and Reaction of CoO: HV Conditions.** To investigate the reactivity of CoO with respect to methanol, CoO was prepared by heating  $\text{Co}_3\text{O}_4$  in a vacuum.<sup>48</sup> The heat treatment was carried out both in

(45) Vohs, J. M.; Barteau, M. A. *Surf. Sci.* **1986**, 176, 91.

(46) Bowker, M.; Houghton, H.; Waugh, K. C. *J. Chem. Soc., Faraday Trans. 1* **1982**, 78, 2573 and references therein.

(47) Kim, K. S.; Barteau, M. A.; Farneth, W. E. *Langmuir* **1988**, 4, 533 and references therein.

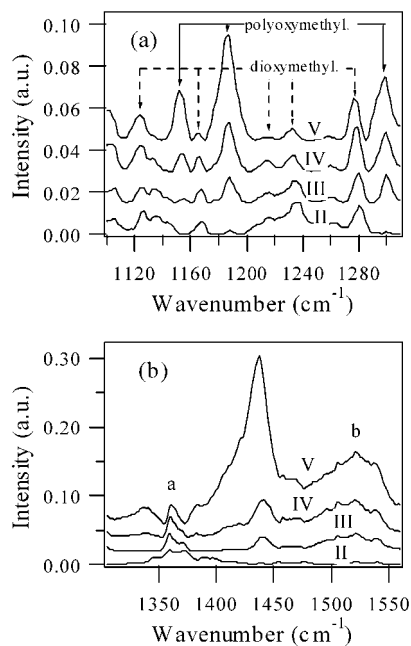


**Figure 6.** DRIFT spectra (Kubelka–Munk units) obtained after exposure of the  $\text{Co}_3\text{O}_4$  powder (calcined at 1023 K) to methanol at the different temperatures (II) 373 K, (III) 423 K, (IV) 473 K, and (V) 523 K: (a) region between 1100 and 1310  $\text{cm}^{-1}$ , (b) region between 1300 and 1560  $\text{cm}^{-1}$ .

**Table 3. FTIR Data ( $\text{cm}^{-1}$ ) of Vapor and Liquid Methanol and Aluminum Methoxide**

assignment	gaseous $\text{CH}_3\text{OH}$	liquid $\text{CH}_3\text{OH}$ <sup>39</sup>	$\text{Al}(\text{OCH}_3)_3$ <sup>41</sup>
C–O stretch	1012 <sup>39</sup> 1034 vs <sup>39</sup> 1060 <sup>39</sup>	1029	1040
O–H bend	1340 <sup>40</sup> 1346 m <sup>39</sup>	1420 m br	
$\text{CH}_3$ bend (a) a''	1430 w <sup>39,40</sup>	1420	
$\text{CH}_3$ bend (s) a'	1455 m <sup>39,40</sup>	1455 m	
$\text{CH}_3$ bend (a) a'	1477 m <sup>39,40</sup>	1480 sh	
$\text{CH}_3$ stretch (s)	2826 2845 s <sup>39</sup> (2844) <sup>40</sup> 2869 <sup>39</sup>	2822 s	2840
$\text{CH}_3$ stretch (a)	2973 vs <sup>39</sup> (2977) <sup>40</sup>	2934 vs	2940
OH stretch	3673 <sup>39</sup> 3687 s <sup>39</sup> (3682) <sup>40</sup> 3713 <sup>40</sup>	3337 vs br	

rough and in high vacuum conditions, and the obtained samples were characterized by means of XPS (Tables 2 and 4).

The heat treatment in rough vacuum was carried out at 523 K, as indicated in Table 4. The BEs of the  $\text{Co} 2\text{p}$  XP peaks (780.4 and 795.6 eV) suggest an unsatisfactory formation of  $\text{CoO}$ .<sup>24,26,28</sup> This consideration is also confirmed by the very low intensity of the shake-up peaks (Figure 9).<sup>14,27,28</sup>

The O 1s XP peak (Figure 10a) is very similar to the O 1s peak of  $\text{Co}_3\text{O}_4$ ; the peak shape reveals the same three components centered at ca. 530.0–530.5, 531.2–531.4, and 532.5 eV.

In the sample heated in HV for 14.5 h at 643 K, the  $\text{Co} 2\text{p}$  shake-up peaks (Table 4) become more evident (Figure 9). The O 1s peak shape changes after this treatment, and the intensity of the components at

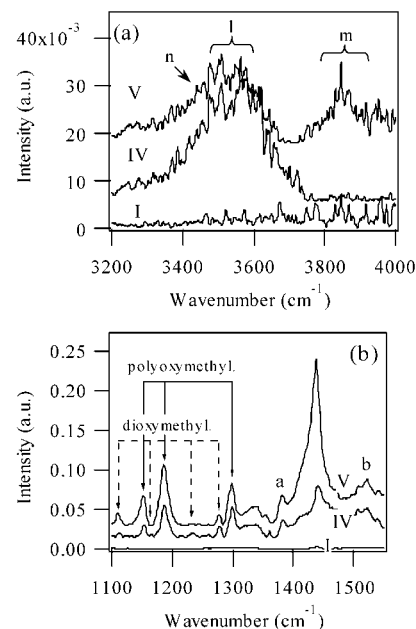


**Figure 7.** DRIFT spectra (Kubelka–Munk units) obtained after exposure of the  $\text{Co}_3\text{O}_4$  powder (calcined at 1023 K) to methanol and successively to  $\text{N}_2$  at the different temperatures (I) RT, (IV) 473 K, and (V) 523 K: (a) region between 3200 and 4000  $\text{cm}^{-1}$ , (b) region between 1100 and 1550  $\text{cm}^{-1}$ .

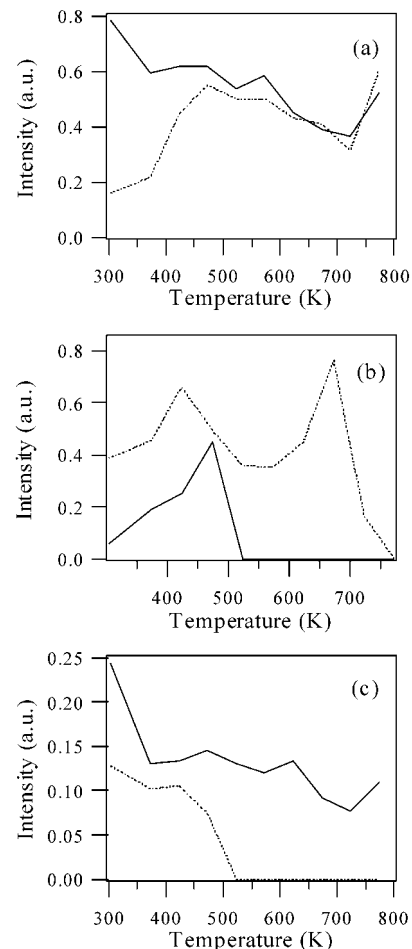


**Figure 8.** Desorption patterns obtained after exposure of the  $\text{Co}_3\text{O}_4$  powder to methanol: (a) (—)  $\text{CH}_3\text{OH}$ , (---)  $\text{CO}/5$ ; (b) (—)  $\text{H}_2\text{O} \times 10$ , (---)  $\text{H}_2$ ; (c) (—)  $\text{CH}_3\text{OCH}_3$ , (---)  $\text{CO}_2$ .

higher BE decreases (Figure 10b). Moreover, the O/Co atomic ratio decreases from 1.3 to 1.0. These results

(48) Gazzoli, D.; Occhiuzzi, M.; Cimino, A.; Cordischi, D.; Minelli, G.; Pinzari, F. *J. Chem. Soc., Faraday Trans.* **1996**, 92, 4567.

**Table 4. XPS Data Obtained on the Cobalt Oxide Powder during the Preparation Procedure of the CoO<sup>a</sup>**

temp (K)	time (h)	shake-up Co 2p <sub>3/2</sub>	shake-up Co 2p <sub>3/2</sub>	shake-up Co 2p <sub>1/2</sub>	shake-up Co 2p <sub>1/2</sub>	O/Co
523	16	780.4	788.1	795.6	804.7	1.3
643	14.5	780.3	786.8	796.2	803.6	1.0
RT <sup>b</sup>	2	780.8	786.7	796.4	803.5	1.1
643	20	780.5	786.7	796.4	804.1	1.0
743	19	781.0	786.8	796.9	803.2	1.0
743	33	781.0	786.9	797.0	803.3	1.0

<sup>a</sup> Sample heated at 523 K was heated under rough vacuum ( $1 \times 10^{-1}$  Pa), whereas all other samples were heated under HV conditions ( $1 \times 10^{-7}$  Pa). <sup>b</sup> Sample indicated as RT was heated at 643 K and exposed to the laboratory atmosphere for 2 h at RT.

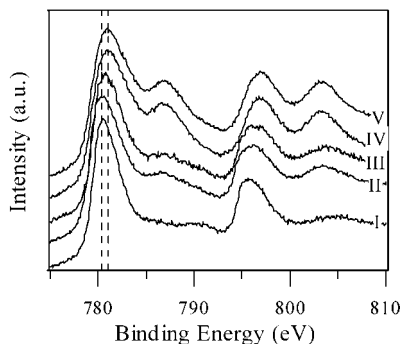


**Figure 9.** Co 2p XP spectra recorded during the preparation of the CoO catalyst powder (heating of the  $\text{Co}_3\text{O}_4$  powder sample under vacuum conditions) after heat treatments (I) under rough vacuum conditions at 523 K for 16 h and (II) under HV conditions at 643 K for 14.5 h and of the (III) sample heated under HV conditions at 643 K for 14.5 h and exposed to the laboratory atmosphere for 2 h; samples heated under HV conditions at (IV) 743 K for 19 h and at (V) 743 K for 33 h. (The spectra are normalized with respect to their maximum values.)

indicate that the heat treatment under HV causes surface reduction, as well as OH group condensation.

In the sample exposed (2 h) to the laboratory atmosphere (Figure 10c), the O 1s components at 531.3 and 532.5 eV increase again, suggesting the ease of surface hydroxylation.<sup>28</sup>

Further heating of the sample (at 743 K) causes an increase in the shake-up peak intensity, as well as a shift in the Co 2p peak toward slightly higher BE (Figure 9 and Table 4). These new values agree with the presence of CoO;<sup>24,26,28</sup> the obtained O/Co atomic ratio (1.0) confirms this result. Moreover, inspection of the O 1s XP peak (Figure 10d) suggests that the OH group contributions further decrease with increasing temperature. Sample heating for longer times and at higher temperatures does not cause any further reduction of the sample surface.

The X-ray induced Auger Co LMM peak (Figure 11) allows for better discrimination between Co(III), the component at lower BE, and Co(II), the contribution at higher BE.<sup>49</sup> The different peak shape obtained after the heat treatment in HV confirms the increased presence of Co(II). It should be considered that the Co(III) contribution is still quite evident, indicating that the reduction involves only a few superficial monolayers. This result is easily explained by the diffusion problems that can be important in the case of a pellet; it is

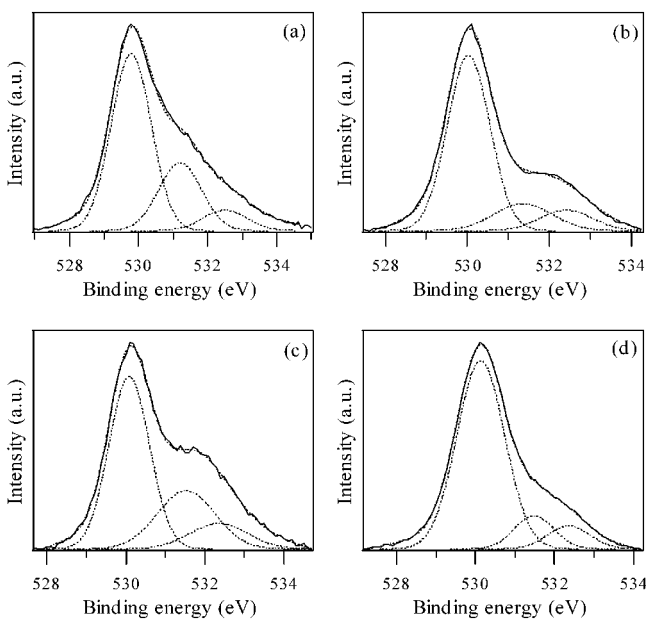


**Figure 10.** O 1s XP spectra obtained during the preparation of the CoO catalyst powder (heating of the  $\text{Co}_3\text{O}_4$  powder sample under vacuum conditions) after heat treatments (a) under rough vacuum conditions at 523 K for 16 h and (b) under HV conditions at 643 K for 14.5 h; (c) of the sample heated under HV conditions at 643 K for 14.5 h and exposed to the laboratory atmosphere for 2 h; and (d) of the sample heated under HV conditions at 743 K for 19 h. (The spectra are normalized with respect to their maximum values; the fitting procedure results are also shown.)

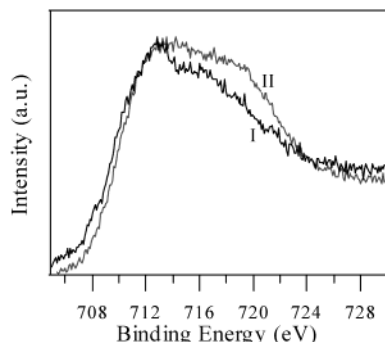


**Figure 11.** Co L<sub>3</sub>M<sub>45</sub>M<sub>45</sub> spectra: (I)  $\text{Co}_3\text{O}_4$  powder sample (calcined at 1023 K), (II) CoO obtained by heating the  $\text{Co}_3\text{O}_4$  powder sample under HV at 743 K for 19 h. (The spectra are normalized with respect to their maximum values.)

noteworthy that, in the present case, this fact does not constitute a problem because we are interested in surface reactivity. An important distinction between  $\text{Co}_3\text{O}_4$  and CoO is also the difference between the binding energy of the Co 2p<sub>3/2</sub> and O 1s peaks, which is greater for CoO than for  $\text{Co}_3\text{O}_4$ , in accordance with literature data.<sup>50</sup>

The obtained CoO sample (heated under HV conditions at 743 K for 19 h) was then exposed to methanol (under HV conditions).

Inspection of the XP spectra recorded after exposure to methanol (Figure 12) indicates that chemisorption at RT or at higher temperature does not modify the peak shape/position or the atomic composition.

(49) Haber, J.; Ungier, L. *J. Electron Spectrosc. Related Phenom.* **1977**, *12*, 305.

(50) Sato, M.; Hara, H.; Kuritani, H.; Nishide, T. *Solar Energy Solar Cells* **1997**, *45*, 43.

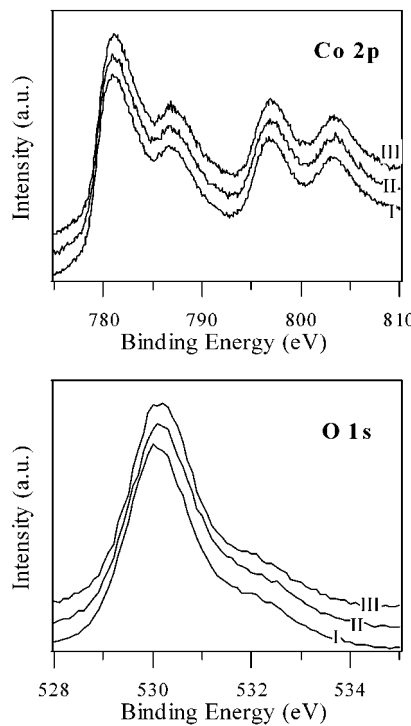


**Figure 12.** Co 2p and O 1s XP spectra of the CoO powder sample (obtained by heating the  $\text{Co}_3\text{O}_4$  sample at 743 K for 19 h): (I) before and after the exposure to methanol at (II) RT and (III) 773 K. (The spectra are normalized with respect to their maximum values.)

The QMS results (Figure 13) indicate that the molecularly chemisorbed methanol desorbs at temperatures lower than ca. 473 K, whereas the dissociatively chemisorbed methanol desorbs between 573 and 723 K.<sup>45–47</sup> The mass spectra suggest that desorption of the molecularly chemisorbed methanol is accompanied by its decomposition to CO and  $\text{H}_2$ ;<sup>19</sup> in fact, these species are evident at temperatures lower than ca. 450 K. The desorption of the dissociatively chemisorbed methanol, in contrast, is accompanied by the formation of CO,  $\text{CO}_2$ , and  $\text{H}_2\text{CO}$ ;<sup>19,37,42,45–47</sup> in particular,  $\text{CO}_2$  is prevalent at lower temperatures (around 573 K) and formaldehyde at higher temperatures (600–700 K). Fragmentation products are present at both low and high temperatures.<sup>46</sup>

## Discussion

The mechanism of interaction between alcohol molecules and oxide surfaces (Scheme 1) depends strongly on the degree of surface hydroxylation. On a dehydroxylated surface, the mechanism can be dissociative (Scheme 1, type I), to produce hydroxyl groups and alkoxy groups, or molecular (Scheme 1, type 2), through the interaction of the alcohol molecules with the Lewis acid and base sites.<sup>51,52</sup> Three additional modes of chemisorption are possible for a hydroxylated surface: esterification with surface hydroxyl groups (Scheme 1, type III), replacement of molecular water present on the surface (Scheme 1, type IV), and reversible adsorption on the surface

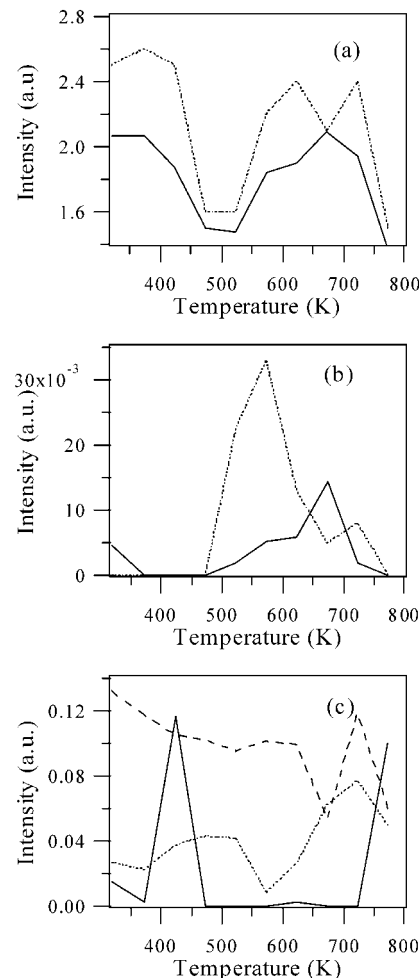


**Figure 13.** Desorption patterns obtained after exposure of the CoO powder to methanol: (a) (—)  $\text{CH}_3\text{OH} \times 2.5$ , (···) CO; (b) (—)  $\text{H}_2\text{CO}$ , (···)  $\text{CO}_2$ ; (c) (—)  $\text{H}_2\text{O}$ , (···)  $\text{CH}_3\text{CH}_2$ , (---)  $\text{CH}_3$  – 0.04.

hydroxyl groups or methoxy groups through hydrogen bonds (Scheme 1, type V).<sup>53</sup> Careful observation of the effect of methanol exposure on the distributions of OH groups and  $\text{H}_2\text{O}$  adsorbed molecules on the oxide surface allows the different interaction mechanisms to be distinguished.<sup>54</sup>

The  $\text{Co}_3\text{O}_4$  surface is only slightly hydroxylated, as demonstrated by the DRIFT and XP spectroscopic results: in fact, in the sample calcined around 1023 K, the presence of OH groups is evidenced only by XPS. In such a situation, the interaction mechanisms involving OH groups (Scheme 1, type III) cannot be significant; it is noteworthy that a mechanism involving OH groups should give rise to a decrement in OH groups and an increment in water molecules, whereas an increment in hydroxyl groups was observed.

Moreover, a comparison between the DRIFT spectra obtained before and after the chemisorption of methanol at room temperature shows that the water contribution does not change as a consequence of the chemisorption: this result allows the replacement of water

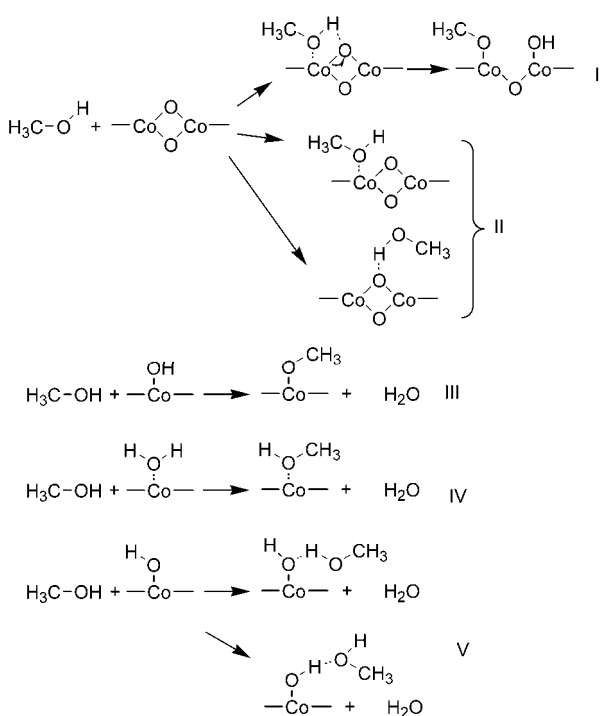
(51) Kung, H. H. *Transition Metal Oxides: Surface Chemistry and Catalysis*; Elsevier: Amsterdam, 1989; Chapter 10.

(52) Thornton, E. W.; Harrison, P. G. *J. Chem. Soc., Faraday Trans. 1* **1975**, 71, 2468.

(53) Suda, Y.; Morimoto, T.; Nagao, M. *Langmuir* **1987**, 3, 99.

(54) It is noteworthy that the DRIFT spectra were collected in Kubelka–Munk units, using as a reference the reflectance spectrum recorded before exposure. This experimental setup allows the effects of the adsorption of methanol to be emphasized.

Scheme 1



molecules by alcohol molecules (Scheme 1, type IV) to be excluded.

For this surface, then, a dissociation mechanism with the formation of hydroxyl and alkoxy groups (Scheme 1, type I) is suggested, with the molecularly chemisorbed methanol arising from an acid/base interaction between the alcohol molecule and the Lewis acid sites distributed<sup>55</sup> on the  $\text{Co}_3\text{O}_4$  powder surface (Scheme 1, type II).

At higher temperatures (423 K), the formation of water is evident after exposure which suggests an interaction mechanism involving OH groups (Scheme 1, type III).

At 523 K, the exposure to methanol causes the formation of new isolated OH groups, suggesting the prevalence of a direct dissociation mechanism involving the Lewis acid/base sites (Scheme 1, type I). In fact, the temperature promotes the condensation of the OH groups, and new acid and base sites appear on the surface,<sup>44</sup> facilitating a direct dissociation mechanism with the formation of new OH groups ( $3800\text{--}3850\text{ cm}^{-1}$ ).

Accordingly, the QMS results show the existence of two nonequivalent methoxy groups whose desorption temperatures are centered around 473 and 573 K.

The strong influence of surface hydroxylation on the interaction mechanisms is also suggested by a comparison with different oxides.<sup>16,17,37</sup>

The oxidation products, mainly formate and polymers of formaldehyde, are evident at temperatures higher than 373 K; they are only slightly bonded to the  $\text{Co}_3\text{O}_4$  surface and can be removed by a nitrogen flow, whereas oxidation products obtained at temperatures higher than 473–523 K are more tightly bonded.

The present results seem to confirm the literature data concerning the mechanism of methanol oxidation on oxide surfaces (Scheme 2).<sup>43,56–60</sup> Methanol reacts

with the surface to form methoxy groups. At higher temperatures, the methoxy groups give rise to the formation of dioxymethylene species that evolve to formate, releasing hydrogen. The formation of polymers of formaldehyde is competitive with the formation of formate.

Interesting observations derive from the results obtained after chemisorption under HV conditions. The desorption of the methoxy species around 473 K is accompanied by the desorption of  $\text{CO}$ ,  $\text{H}_2\text{O}$ ,  $\text{H}_2$ , and  $\text{CO}_2$ .  $\text{CO}$  and  $\text{H}_2$  can derive from the decomposition of the methoxy groups, whereas the presence of  $\text{CO}_2$  agrees with the formation of dioxymethylene intermediate. At higher temperatures,  $\text{CO}_2$  and  $\text{H}_2\text{O}$  no longer desorb. This result can be related to the surface reduction caused by the heat treatment under HV and by the reaction path. In fact, the oxygen deficiency can unfavor the formation of dioxymethylene species; as a consequence the desorption products can only derive from the decomposition of the methoxy species. In this respect the absence of coordinatively unsaturated oxygen species should make the oxide surface selective with respect to the dehydrogenation reaction and then to the formation of formaldehyde (or polymers of the formaldehyde).

It has to be considered that oxygen-deficient oxide surfaces can break down carbon dioxide, giving rise to carbon monoxide.<sup>61,62</sup>  $\text{CO}_2$  conversion to  $\text{CO}$  (Scheme 3) might thus be due to the  $\text{Co}(\text{II})$  species formed on the powder surface.

The presence of hydrocarbons and ethers between the desorption products observed upon exposure of  $\text{CoO}$  (prepared under HV conditions) to methanol suggests the capability of the  $\text{CoO}$  surface to break the  $\text{CH}_3\text{--OH}$  bond.

The degree of surface hydroxylation and the distribution of acid/base sites, determine the mechanism of interaction between the alcohol and the oxide surface and then the formation of methoxy groups. The exposed oxygen species can give rise to the possible formation of dioxymethylene moieties and influence the possible products: formate and carbon dioxide derive from the dioxymethylene, whereas formaldehyde and formaldehyde polymers can form from the methoxy groups.

In general, the oxidizing power of a metal oxide surface can be associated with the strength of the metal–oxygen bond and with the possibility of incorporating molecular oxygen into the crystal lattice, i.e., the ability to reoxidize the reduced active sites with gaseous oxygen. In contrast, the absence of weakly bonded oxygen species might be fundamental in determining the reaction path and then the catalyst selectivity. Moreover, the strong influence of the acid/base character of the surface in determining the activity in oxidation reaction has to be considered,<sup>60,63,64</sup> as dem-

(57) Hussein, G. A.; Sheppard, N.; Zaki, M. I.; Fahim, R. B. *J. Chem. Soc., Faraday Trans.* **1991**, *87*, 2655.

(58) Hussein, G. A.; Sheppard, N.; Zaki, M. I.; Fahim, R. B. *J. Chem. Soc., Faraday Trans.* **1991**, *87*, 2661.

(59) Lietti, L.; Tronconi, E.; Forzatti, P. *J. Mol. Catal.* **1988**, *44*, 201.

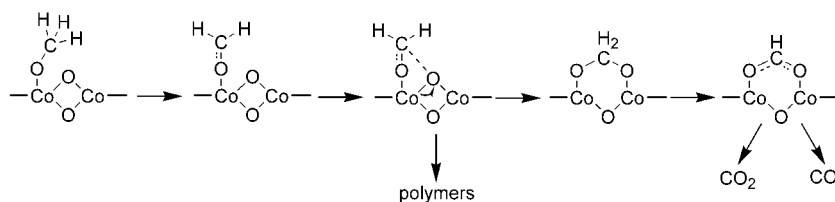
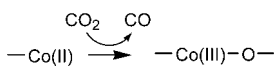
(60) Ai, M. *J. Catal.* **1983**, *83*, 141.

(61) Casarin, M.; Falcomer, D.; Glisenti, A.; Vittadini, A.; to be published on the *Chem-Eur. J.*

(62) Raupp, G. B.; Dumesic, J. A. *J. Phys. Chem.* **1985**, *89*, 5240.

(63) Ai, M. *J. Catal.* **1977**, *49*, 313.

(64) Ai, M. *J. Catal.* **1989**, *120*, 206.

**Scheme 2****Scheme 3**

onstrated by the reactivity of the  $\text{Fe}_2\text{O}_3$  with respect to methanol.<sup>37</sup> In our opinion, the distribution of the acid/base sites can deeply influence the mechanism of interaction between the reagents and the catalysts as well as the possibility of activating the reagent. In the present case, the presence of coordinatively unsaturated oxygen species allows for the formation of dioxymethylene, which determines the reaction path and the selectivity of the catalyst.

Further work is in process in our laboratory to better identify the sites responsible for the methanol interaction, as well as the acid/base and redox sites whose presence can influence the reaction path.

### Conclusions

In this paper, the interaction between cobalt oxides and methanol was studied.  $\text{Co}_3\text{O}_4$  was prepared by precipitation from aqueous solution and calcination in air, whereas  $\text{CoO}$  was obtained by heating the  $\text{Co}_3\text{O}_4$  powder under HV conditions.

The  $\text{Co}_3\text{O}_4$  powder samples were characterized by means of XP and DRIFT spectroscopic techniques, XRD, and thermal analysis, whereas  $\text{CoO}$ , obtained under HV conditions, was studied by means of XPS.

The interaction between  $\text{Co}_3\text{O}_4$  and methanol was studied both at atmospheric pressure (by means of DRIFT spectroscopy) and under HV conditions (by means of XPS and QMS), whereas the chemisorption of methanol on the  $\text{CoO}$  surface was studied only under HV conditions.

Methanol chemisorbs mainly molecularly on the  $\text{Co}_3\text{O}_4$  surface. Dissociation of the alcohol is more evident at 373 K and occurs through two different mechanisms: direct dissociation is prevalent at low and high temperatures, whereas dissociation by interaction with the hydroxyl groups present on the surface is prevalent at intermediate temperatures (400–500 K). This behavior is probably a consequence of the distribution and strength of the acid/base sites on the  $\text{Co}_3\text{O}_4$  surface.

Around 373 K, the formation of formate and dioxymethylene species is evident, followed, around 423 K, by the formation of polyoxymethylene. These species in-

teract more strongly than methanol with the oxide surface and do not decompose to carbon oxides.

In fact this oxide shows a better selectivity than other oxides.  $\text{NiO}$ ,<sup>16</sup> as an example, shows the formation of formate at 423 K, but  $\text{CO}_2$  is already evident at 323 K.  $\text{WO}_3$ , another extensively used catalyst (olefin oxidation, olefin metathesis),<sup>65–69</sup> interacts with methanol, giving rise to formic acid and  $\text{CO}_2$  at temperatures higher than 423 K.<sup>70</sup>

Methanol interacts molecularly and dissociatively with the  $\text{Co}_3\text{O}_4$  surface under HV conditions. Molecularly chemisorbed methanol desorbs at temperatures lower than about 373 K, whereas the methoxy groups desorb at 473 and 573 K. The desorption of molecularly chemisorbed methanol is accompanied by the desorption of  $\text{CO}_2$  and of fragmentation/recombination products (dimethyl ether and ethyl methyl ether). At higher temperatures, the desorption of methoxy groups is accompanied mainly by the presence of CO.

Mass spectra suggest, in the case of  $\text{CoO}$ , that desorption of the molecularly chemisorbed methanol is accompanied by its decomposition to CO and  $\text{H}_2$ . Desorption of the dissociatively chemisorbed methanol is accompanied by the formation of CO,  $\text{CO}_2$ , and  $\text{H}_2\text{CO}$ , with the  $\text{CO}_2$  being prevalent at lower temperatures and the formaldehyde at higher temperatures.

DRIFT and QMS results allow us to hypothesize a mechanism for the interaction between methanol and the cobalt oxide surfaces and for the oxidation of the alcohol.

**Acknowledgment.** The authors gratefully acknowledge Professor E. Tondello for helpful discussions and Professor P. Colombo for the XRD measurements.

CM0211150

- (65) De Rossi, S.; Iguchi, E.; Schiavello, M.; Tilley, R. J. D. *Z. Phys. Chem. Neue Folge* **1976**, *103*, 193.
- (66) Schiavello, M.; Pepe, F.; Cannizzaro, M.; De Rossi, S.; Tilley, R. J. D. *Z. Phys. Chem. Neue Folge* **1977**, *106*, 45.
- (67) Haber, J.; Janas, J.; Schiavello, M.; Tilley, R. J. D. *J. Catal.* **1983**, *82*, 395.
- (68) Van Roosmalen, A. J.; Mol, J. C. *J. Catal.* **1982**, *78*, 17.
- (69) Rodriguez, I.; Guerrero-Ruiz, A.; Homs, N.; Ramirez de la Piscina, P.; Fierro, J. L. G. *J. Mol. Catal. A: Chem.* **1995**, *95*, 147.
- (70) Tocchetto, A.; Glisenti, A. *Langmuir* **2000**, *16*, 6173.
- (71) McIntyre, N. S.; Johnston, D. D.; Coastworth, L. L.; Davidson, R. D. *Surf. Interface Anal.* **1990**, *15*, 265.
- (72) Jiménez, V. M.; Fernandez, J. P.; Espinós, J. P.; González-Elipe, A. R. *J. Electron Spectrosc. Related Phenom.* **1995**, *71*, 61.
- (73) Strydom, C. A.; Strydom, H. J. *Inorg. Chim. Acta* **1989**, *159*, 191.